

Thermal based functional evaluation of urban park vegetation

John Bosco NJOROGE, Akihiro NAKAMURA, Yukihiro MORIMOTO

Department of Regional Environmental Science, Osaka Prefecture University, 1-1 Gakuen-cho, Sakai 599 - 8531, Japan

Abstract—An evaluation of the urban park vegetation was conducted by integrating airborne multispectral scanning system (MSS) thermal band data with meteorological. MSS data acquired in the morning and afternoon were utilized to assess the radiant energy budget of different ground cover types and its relationship with the surface types. The spatial distribution of surface temperature (T_s) and surface albedo (A) varied between different surfaces. However, the spatial variability of net radiation (R_n) was reduced by negative feedback of A - T_s relationship. The Normalized Difference Vegetation Index (NDVI) had a negative correlation with T_s but positively correlated to R_n of the different surface types. Thermal response number (TRN), which expresses the dissipative behavior of radiant energy, correctly characterized each ground cover type according to the validated surface property. Forested and lawn covered sites had the highest TRN values consistent with their tendency to resist microclimatic change. The approach shows that by utilizing the MSS thermal signatures, we can relate the microenvironment processes to the biophysical character of each site offering an opportunity to diagnose site-specific problems. The approach is proposed as a direct and easily adaptable method for monitoring the urban green park areas and for making objective decisions about their management.

Keywords: surface temperature, surface property, radiant energy, TRN.

1 Introduction

Comprehensive methods for evaluation of the urban park vegetation are necessary in order to solve many of the problems facing managers of urban park vegetation. Many restoration work through planting have been reported (Lassini, 1993). The revegetative areas become of great ecological value within the suburban ecotopes (Naveh, 1998) and they should be managed objectively. Spatial information relating microclimatic processes to all elements within such landscapes is essential for monitoring purposes.

The heterogeneity of ground covers across the landscape results to a contrast of temperatures creating energy gradients and spatial discontinuity of microclimates in the landscape. Because thermal infrared (TIR) measurements are indicative of net surface energy balance, they are an important source of ground information such as surface wetness, canopy stress conditions and evapotranspiration rates (Price, 1989). In this study we explore the thermal conditions of different ground cover types within an urban park using airborne MSS thermal band data. The objectives are to estimate the spatial distribution of surface temperature (T_s), surface albedo (A), net radiation flux (R_n) and to quantify each surface type according to its surface properties.

2 Materials and methods

2.1 Study area and data processing

The study area is the reclaimed site of Expo '70 park that was converted into a forested park after revegetation with indigenous plant species. It is located in Osaka Prefecture in Suita City, within latitudes 34°47' and 34°48'N and longitudes 135°31' and 135°32'E with a mean altitude of 50.5m above sea level. The zone is highly urbanized and the park has multipurpose uses of recreation, education and conservation.

MSS data sensed on October 3 (14:10 pm) and October 7 (09:12 am), 1995 represented the afternoon (pm) and morning (am) conditions, respectively. Since landscape processes are a function of scale and the resolving capability of the sensor (Nellis, 1989), sensor resolution of

2.5m was selected for the objectives of this analysis. Image processing was done using ERDAS software (ERDAS, 1991). Data generated was used to obtain the ground cover classification, surface albedo, surface temperature and vegetation amount.

Supervised image classification supported by the field validation was conducted using 6 bands. Parametric decision rule was applied as the algorithm for classification and 12 ground cover types identified (Fig.1).

2.2 Surface temperature and albedo

The thermal infrared band 11 (8.0—14.0μm) of MSS was utilized to calculate the radiometric surface temperature. Ground surface temperatures, recorded simultaneously with aircraft overpass were used to calibrate the radiometric brightness. Correction for surface temperature was done using the Stefan-Boltzmann Law and then regressed with corresponding digital values of band 11 to give a linear relationship expressed as,

$$T_B = a_0 + a_1 V_{11},$$

where T_B is the black body temperature, V_{11} is the digital number of band 11, a_0 and a_1 are coefficients of regression (Fig. 2). The surface temperatures (T_s) for each kind of ground cover were obtained by conversion using the Stefan-Boltzmann Law including the emissivity ϵ for each ground cover (k) as,

$$\epsilon k \sigma T_s^4 = \sigma T_B^4,$$

where σ is the Stefan-Boltzmann constant.

The computation of albedo (A) is necessary due to contrasts among different surfaces that directly influences the energy budget. Albedo was calculated from the ratio of outgoing irradiance (absolute radiometric brightness, R_o) to that of the incoming irradiance (R_i). Because some MSS bands lie in the water absorption range, the effect of water vapor absorption was corrected using the method of Lacis and Hansen (Lacis, 1973).

$R_o (W/(sr \cdot m^2))$ for band k ($k = 4-9$, except band 6) detected by the sensor was calculated by

$$R_o = Dk/255 (R_{maxk} - R_{mink}) + R_{mink},$$

where Dk is the DN value of band k , R_{maxk} and R_{mink} are the maximum and minimum measurable radiances of the sensor for band k , respectively. Total irradiance detected by the sensor was expressed as ΣR_o . R_i was expressed as the global solar radiation (R_s) considering the proportion of the whole spectrum covered by the MSS bands.

The normalized difference vegetation index ($NDVI$) was selected as the measure of vegetation in the Expo '70 park. $NDVI$ is defined as

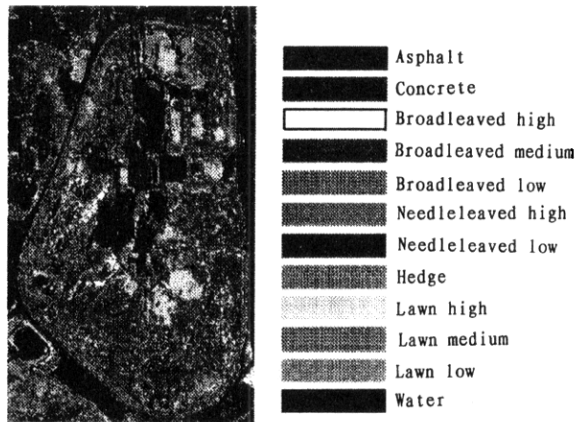


Fig. 1 Results of ground cover classification based on surface properties at the study site

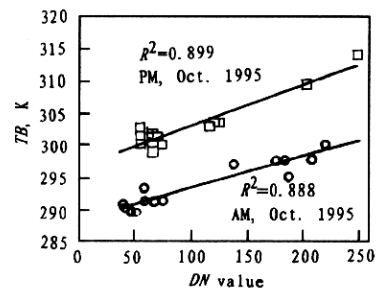


Fig. 2 Relationship between black body temperature (T_B) and digital number (DN) of MSS thermal band 11 used for calibration of ground surface temperatures

$$NDVI = (NIR - R)/(NIR + R),$$

where *NIR* and *R* are reflectance's in the near-infrared and red bands, respectively. *NDVI* indicates the spectral response pattern of vegetation and is useful for quantitative determination of plant vitality and health condition.

2.3 Radiation budget and thermal response

Net radiation (*R_n*) for each surface was derived using the surface energy balance equation given as:

$$R_n = R_s(1 - A) + \epsilon R_L - \epsilon \sigma T_s^4,$$

where *R_s* is the incoming short wave radiation, *A* the surface albedo, and *R_L* the incoming long wave radiation. In order to account for variation in accumulated radiant energy between am and pm, a surface property called thermal response number (*TRN*) was computed for each surface type according to Luvall and Holbo (Luvall, 1991). It is expressed as

$$TRN = \Sigma R_n \cdot \Delta t / \Delta T,$$

where $\Sigma R_n \cdot \Delta t$ represents the total amount of net radiation for that surface between the am and pm flights ($\Delta t = t_2 - t_1$) and ΔT is the change in mean temperature (*T*). Since the expression indicates the rate of change in *T_s* in response to changing thermal fluxes, it also reveals how the nonradiative fluxes of sensible and latent heat react to changing radiant energy inputs.

3 Results

3.1 Surface albedo and temperature

The mean surface albedo for each type of ground cover is shown in Table 1. The albedo varied diurnally with maximum values in the morning and minimum values in the afternoon. Similar observations have been reported by Rosenberg *et al.* (Rosenberg, 1983). The lowest albedo was observed from open water followed by forested areas and was the highest in concrete and grass covered areas. Low surface albedos observed in sites of healthy vegetation was related to higher absorption of short-wave radiation than in low quality vegetation.

Table 1 The mean values of *A*, *T_s*, *NDVI*, *R_n* for each type of ground cover

Ground cover type	<i>A</i>		<i>T_s</i> , °C		<i>NDVI</i>		<i>R_n</i> , W/m ²	
	am	pm	am	pm	am	pm	am	pm
Asphalt	0.17	0.14	23.64	42.00	-0.05	-0.05	158.47	350.92
Concrete	0.17	0.14	20.48	35.86	-0.01	0.03	176.17	395.10
BL high	0.08	0.08	17.72	26.76	0.42	0.46	223.51	488.23
BL medium	0.11	0.09	18.11	28.18	0.43	0.46	209.87	470.62
BL low	0.09	0.10	18.22	30.80	0.29	0.25	217.44	450.74
NL high	0.15	0.10	18.97	29.02	0.41	0.40	192.62	461.82
NL medium	0.15	0.12	19.51	31.65	0.45	0.34	187.66	428.51
Hedge	0.15	0.11	19.66	31.91	0.25	0.32	187.70	435.21
Lawn high	0.17	0.12	19.40	28.99	0.63	0.52	189.93	452.86
Lawn medium	0.21	0.17	21.78	33.71	0.46	0.43	160.92	394.23
Lawn low	0.19	0.16	20.99	34.57	0.20	0.23	173.42	393.72
Open water	0.06	0.05	19.51	25.25	-0.44	-0.36	218.78	514.35

Notes: *A*: surface albedo; *T_s*: surface temperature; *NDVI*: normalized difference vegetation index; *R_n*: net solar radiation; BL: broadleaved; NL: needleleaved

Surface temperature distribution patterns for each cover type were distinct and warmer at pm than am (Table 1). The presence of vegetation influenced the distribution significantly. In healthy vegetation, e. g. broad-leaved forests (high), *T_s* was low indicating high transpiration rates. Therefore, this evapotranspiration energy was not available to raise air temperature. On the hand, in sites of less vigorous and stressed vegetation *T_s* was high due to closure of the stomata resulting to rise in *T_s* in response to the need to dissipate more energy as sensible heat. It is supposed that

the partitioning of R_n shifts from latent to sensible heat under water stress conditions.

3.2 Vegetation index

The mean $NDVI$ values for the different classes are shown in Table 1. $NDVI$ was negatively correlated to T_s and positively correlated to R_n (Fig. 3). The T_s - $NDVI$ index correlation has been attributed to latent heat flux and canopy resistance to transpiration (Carlsson, 1994). Sites of low quality vegetation (e. g. BL (low)) had lower $NDVI$ values in the afternoon than in the morning. $NDVI$ which indicates vegetation activities appears to be very sensitive of change in T_s in response to water deficits created within the leaf surface due to changes in atmospheric demand.

3.3 Net radiation and thermal response

Solar loading was the highest in water, followed by forested lawn sites (Table 1). Variability in solar loading between the plant categories is thought to indicate differences in the surface properties of the biomass, soil water status, and stomatal activity. More active chlorophyll in healthy, vegetation results in more absorption of short-wave radiation (PAR) than less healthy plants. However, spatial variability of R_n between surfaces could be reduced by the negative feedback of the surface albedo-temperature. To circumvent the problem we applied the thermal response number (TRN) concept that reveals the combined influences of surface properties on the microclimate.

Each cover type produced a different TRN value. TRN differentiated between the good and bad quality sites of even similar vegetation types, allowing ranking of surface types as illustrated in Table 2. Although different cover types had almost the same temperature, variation in site-specific biophysical properties that influence energy disposition could be indicated by the TRN value. High TRN values corresponded to small change in T_s between am and pm (Fig. 4). TRN was the highest in water areas. TRN for forested sites was much greater than for lawn, concrete and Asphalt sites consistent with their tendency to exhibit moderated microclimates more than lawn covered areas. Concrete and Asphalt sites had small $TRNs$, indicating little capacity to resist microclimate extremes. Sites of healthy vegetation

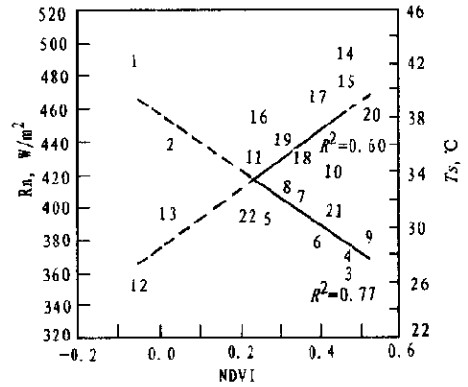


Fig 3 $NDVI$ as a function of net radiation (R_n) and surface temperature (T_s). (1-11) and (12-22) represent Asphalt, Concrete, BL high, BL medium, BL low, NL high, NL medium, Hedge, Lawn high, Lawn medium, Lawn low for R_n and T_s , respectively

Table 2 Surface ranking based on thermal response number (TRN) for each of the ground cover types at the study area

Ground cover type	R_n , W/m^2	T_s , $^{\circ}C$	T_p , $^{\circ}C$	TRN , $kJ/(m^2 \cdot ^{\circ}C)$
Open water	4590	22.38	5.74	2877
Broadleaved (high)	4506	22.24	9.04	1793
Broadleaved (medium)	4416	23.15	10.08	1577
Lawn (high)	4192	24.20	9.58	1575
Needleleaved (high)	4368	24.00	10.05	1565
Needleleaved (medium)	4310	25.58	12.14	1278
Broadleaved (low)	4453	24.51	12.58	1274
Hedge	4332	25.79	12.25	1273
Lawn (medium)	4029	27.74	11.93	1216
Lawn (low)	4075	27.78	13.57	1081
Concrete	4202	28.17	15.37	984
Asphalt	4166	32.82	18.36	817

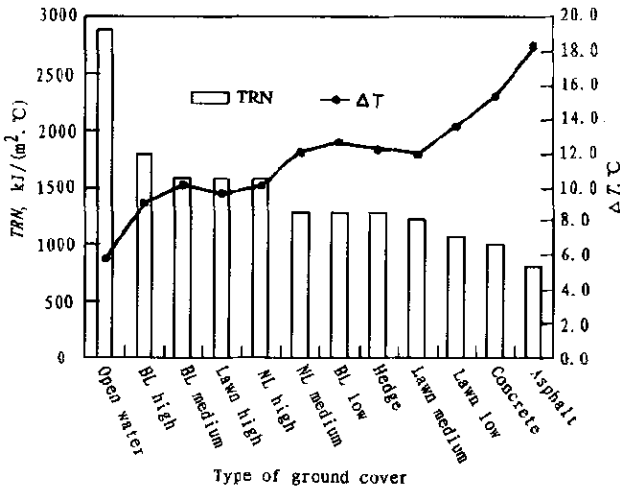


Fig. 4 Thermal response number (*TRN*) relationship with change in temperature (ΔT) for different ground cover types at Expo '70 park (BL = Broadleaved, NL = Needleleaved)

estimated. Therefore, based on the scenario proposed for each site, management practices can be altered accordingly to achieve the set objectives.

Successful rehabilitation of reclaimed and vegetated sites depends on comprehensive methods for monitoring. In addition to the commonly used *NDVI* index, our approach shows that using thermal signatures of airborne *MSS* data, we can relate the micro-environment processes to the biophysical character of each site in the study area. *TRN* correctly characterized the influence of surface properties controlling microclimatic processes giving a unique opportunity to objectively evaluate and manage site-specific problems. Further work on the distribution of the energy terms could improve our understanding about the functional processes. Because of the great ecological value of vegetated sites, thermal based evaluation procedures should be adopted as a tool for monitoring park vegetation in urban ecological planning.

Acknowledgments—We would like to thank Dr. Y Aono, and Dr. X Zhang of the Laboratory of Atmospheric Environment, Osaka Prefecture University for their valuable advice and management of the Expo '70 park for providing the research site.

References

- Carlson T N, Gillies R R, Perry E M, 1994. *Remote Sens Euv*, 9: 161—173
- ERDAS, 1991. *ERDAS Field Guide*. Erdas, Atlanta, GA
- Lacis A A, Hansen J E, 1973. *J Atmos Sci*, 31: 118—133
- Lassinì P, Ballardini P, Mambriani A, Monzani F, 1993. *Landscape and Urban Planning*, 23: 221—231
- Luvall J C, Holbo H R, 1991. *Quantitative methods in landscape ecology* (Eds. by Turner M G, Gardner R H). Berlin: Springer-Verlag. 127—152
- Naveh Z, 1998. *Restoration Ecology*, 6: 135—143
- Nellis M D, Briggs J M, 1989. *Landscape Ecology*, 2: 93—100
- Price J C, 1989. *Theory and applications of optical remote sensing* (Ed. by Asrar G). New York: Wiley. 578 603
- Rosenberg N J, Blad B L, Verma S B, 1983. *Introduction to micrometeorology*. Academic Press Inc. 21—48

had greater *TRNs* than bad sites due to their resistance to microclimate changes.

4 Conclusion

The use of thermal band data coupled with meteorological data had several advantages: (1) The spatial pattern of the ground cover features and their corresponding attributes of *T_s*, radiation balance, and *TRN* could be presented much more clearly with images which have much more visual impact, are more objective and easier to understand. (2) By comparing different surfaces according to their resistance to microclimate changes, the biophysical processes influencing each surface could be